Chemical Engineering Science 64 (2009) 4657–4667

Contents lists available at ScienceDirect

Chemical Engineering Science

journal homepage: www.elsevier.com/locate/ces

Wetting of hydrophobic substrates by nanodroplets of aqueous trisiloxane and alkyl polyethoxylate surfactant solutions

Jonathan D. Halverson[a], Charles Maldarelli[a,b], Alexander Couzis[a], Joel Koplik[b,c,*]

[a]Department of Chemical Engineering, City College of New York, New York, NY 10031, USA
[b]Benjamin Levich Institute for Physico-chemical Hydrodynamics, City College of New York, New York, NY 10031, USA
[c]Department of Physics, City College of New York, New York, NY 10031, USA

ARTICLE INFO

Article history:
Received 2 September 2008
Received in revised form 6 May 2009
Accepted 7 May 2009
Available online 18 May 2009

Keywords:
Superspreading
Simulation
Surfactant
Drop
Interface
Hydrodynamics

ABSTRACT

Trisiloxane surfactants at low concentrations promote the complete and rapid wetting of aqueous droplets on very hydrophobic (hydrocarbon) substrates. This behavior has not been demonstrated by any other surfactant which explains why the trisiloxanes are referred to as superspreaders. Despite many experimental and theoretical investigations the mechanism of superspreading is not fully understood. Molecular dynamics simulations using all-atom force fields have been conducted to attempt to elucidate the mechanism of superspreading. Spherical nanodroplets containing approximately 10,000 water molecules in the bulk and 475 surfactant molecules at the liquid–vapor interface were placed in the vicinity of a graphite substrate and allowed to spread freely at room temperature. In the trisiloxane case the droplet was found to spread very little, although randomly removing 175 surfactant molecules lowered the final contact angle from 110° to 80°. In contrast, an alkyl polyethoxylate surfactant-laden droplet was found to spread significantly further, with the equilibrium contact angle reaching 55°. Similar results for the two surfactant systems were found for cylindrical nanodroplets spreading on a self-assembled monolayer (SAM). The reasons for the lack of spreading in the trisiloxane case and the simulation challenges associated with these systems are discussed. In support of our arguments we demonstrate that the surfactant molecules of an initially uniform aqueous trisiloxane solution self-assemble into a bilayer in tens of nanoseconds on a graphite substrate. Lastly, in a final set of simulations, neat trisiloxane droplets at 450 K are found to arrange into a layered structure on a methyl-terminated SAM and to form a sand pile-shape on a hydroxyl-terminated SAM.

© 2009 Elsevier Ltd. All rights reserved.

1. Introduction

When a small drop of water is placed on a clean glass surface the drop will spread spontaneously until it forms a film of microscopic thickness. If the drop were placed on a surface that had been coated with Teflon® (e.g., a non-stick cooking pan) a qualitatively different behavior would be observed. Instead of wetting the surface the water drop would form a spherical cap with a well-defined contact angle of 110°. The Young equation relates the interfacial tensions or surface energies to the contact angle:

$$\gamma_{SV} = \gamma \cos\theta + \gamma_{SL}, \tag{1}$$

where γ_{SV} is the solid–vapor surface energy, γ is the liquid–vapor surface energy, γ_{SL} is the solid–liquid surface energy, and θ is the macroscopic equilibrium contact angle.

Various industrial wetting processes call for aqueous solutions to spread on difficult-to-wet surfaces. One example from the agrochemical industry is the application of pesticides to plant leaves, which are difficult-to-wet due to their waxy coating. When these solutions are applied, instead of spreading on the leaf as desired, they tend to form beads which subsequently roll off of the leaf. This limitation is overcome by the addition of surface-active agents or surfactants to the solution which reduce the interfacial tensions and increase the wetted area (Knoche, 1994). Surfactants are also used to enhance wetting in the printing, cosmetics, and painting industries.

Surfactants enhance the wetting of aqueous solutions on difficult-to-wet surfaces by adsorbing at the liquid–vapor and solid–liquid interfaces. This leads to a reduction in the interfacial tension of each interface. According to Eq. (1), a decrease in γ and γ_{SL} corresponds to a decrease in the equilibrium contact angle (when θ is initially less than 90°). The wetting of smooth solids by pure, simple liquids

* Corresponding author at: Benjamin Levich Institute for Physico-chemical Hydrodynamics, City College of New York, New York, NY 10031, USA. Tel.: +1 212 650 8162; fax: +1 212 650 6835.
E-mail address: koplik@sci.ccny.cuny.edu (J. Koplik).

0009-2509/$ - see front matter © 2009 Elsevier Ltd. All rights reserved.
doi:10.1016/j.ces.2009.05.010

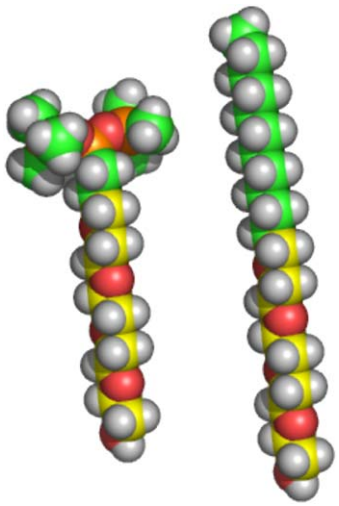

Fig. 1. (Left) M(D′E_4OH)M and (right) $C_{12}E_4$ shown in all-trans configurations. In aqueous solution the hydrophilic groups of these molecules form a structure that resembles a helix while the hydrophobes tend to remain in the all-trans configuration. Methyl and methylene groups of the hydrophobe are shown as green, methylene of the hydrophile is yellow, silicon is orange, oxygen is red, and hydrogen is white. All molecular graphics in this work were created using PyMol (DeLano, 2002). (For interpretation of the reference to color in this figure legend, the reader is referred to the web version of this article.)

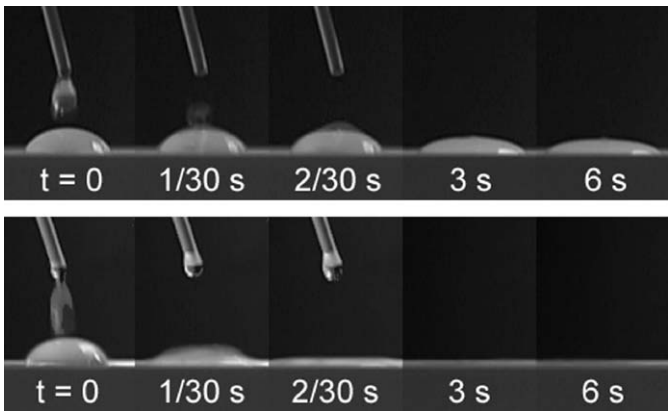

Fig. 2. (Top) A small quantity of alkyl polyethoxylate/alcohol solution is added to a sessile water drop on a solid substrate of moderate hydrophobicity (polycarbonate). The aqueous surfactant solution is $C_{12}E_8$ at seven times the critical aggregation concentration (CAC) and $C_{12}E_0$ at 21 times the solubility limit. The initial base diameter of the drop is approximately 1 cm. (Bottom) A trisiloxane solution is added to a sessile water drop. The superspreading solution is >60 wt% methyl (propylhydroxide, ethoylated) bis(trimethylsiloxy) silane, 15–40 wt% polyethylene oxide monoallyl ether, ≤ 9 wt% polyethylene glycol at 20 parts water to 1 part solution by volume.

is well understood (de Gennes, 1985). However, when additives are present the situation becomes more complicated.

A trisiloxane superspreading surfactant is shown in Fig. 1. The shorthand notation for these surfactants is M(D′E_n)M, where M is $(CH_3)_3SiO-$, D′ is $(CH_3)Si(CH_2)_3-$, and E_n is $-(OCH_2CH_2)_nOR$ with R typically being $-H$, $-CH_3$, or $-CH_2CO_2H$. The hydrophobe of these surfactants is a methyl-terminated trisiloxane group, MD′M, which has approximately the same hydrophobicity (as judged by the phase behavior) as a C_{12} chain (He et al., 1993). The chemical formula for the alkyl polyethoxylate surfactants in shorthand notation is C_mE_n, where C_m is $CH_3(CH_2)_{m-1}-$. A $C_{12}E_4$ molecule with the same hydrophile as M(D′E_4OH)M is shown in Fig. 1.

Fig. 2 illustrates the superior wetting properties of the trisiloxane surfactants. A small quantity of a conventional surfactant solution is added to a sessile water drop. With time the surfactant causes a decrease in the contact angle by tens of degrees but complete wetting is not seen. When the experiment is repeated with a superspreading solution the sessile drop is found to completely wet the surface in less than a second.

While the mechanism of superspreading has remained unexplained since its discovery in the 1960s (Schwartz and Reid, 1964) much has been learned through experimental investigation (Hill, 1998). An early study by Ananthapadmanabhan et al. (1990) considered three silicone surfactants including M(D′E_8OCH_3)M. The trisiloxane surfactant gave the best wetting results. The authors speculated that superspreading was due to the ability of the trisiloxane surfactant molecules to reduce the liquid–air surface tension to low values, a high affinity of the surfactants for low energy substrates, fast adsorption kinetics at the liquid–vapor and solid–liquid interfaces, and a favorable molecular orientation at the spreading edge. Zhu et al. (1994) investigated the wetting of six silicone surfactants on Parafilm® and found that the four that gave a dispersed surfactant-rich phase were the ones that exhibited superspreading. The authors speculated that a thin, high tension film may be present at the leading edge of the drop. Such a film would suggest that superspreading is driven by the Marangoni effect. Of the various linear and hammer-like alkyl polyethoxylate surfactants considered none were found to be superspreaders.

A number of studies have explored the link between superspreading and surfactant phase behavior. Gradzielski et al. (1990) examined the aqueous phase behavior of various siloxane surfactants. Scriven and coworkers investigated the phase behavior of M(D′E_nOH)M/H_2O for $n=5$, 8, 12, and 18 using a variety of experimental techniques (He et al., 1993). For the same value of n, the phase behavior between the trisiloxanes and the alkyl polyethoxylates was found to be similar. Hill et al. (1994) studied the aqueous phase behavior of M(D′E_8OH)M, M(D′E_8OCH_3)M, and M(D′E_8OAc)M. The terminal group, R, was found to be important. A linear surfactant with a trisiloxane hydrophobe (MDM′E_8OH, where D is $-OSi(CH_3)_2-$ and M′ is $-OSi(CH_3)_2(CH_2)_3-$) was shown to superspread at 0.1 wt% on Parafilm®. This provides further evidence that the hammer-like geometry does not uniquely explain superspreading. Additional studies have determined phase transition temperatures (Wagner et al., 1999b) and binary (Li et al., 1999a, b) and ternary (Kunieda et al., 1998; Wagner et al., 1999b) phase diagrams.

The wetting of M(D′E_nOR)M and C_mE_n surfactant solutions on self-assembled monolayers of varying surface energy has been investigated (Stoebe et al., 1996, 1997a, c). While the trisiloxanes were shown once again to be the only surfactants to cause complete wetting of aqueous drops on highly hydrophobic substrates, the two surfactant classes gave similar qualitative and quantitative results for moderately hydrophobic substrates. The authors referred to this phenomena as surfactant-enhanced spreading. An aqueous M(D′E_8OH)M drop at a concentration of 0.6 wt% on a substrate with a water contact angle of 66° gave a spreading rate of 90 mm^2/s. Similarly, an aqueous $C_{12}E_3$ drop at a concentration of 0.2 wt% on a substrate with a water contact angle of 53° gave a spreading rate of 85 mm^2/s. These are the maximum values reported for each class. Humidity was shown to be less important as suggested by Zhu et al. (1994). Ionic surfactants have been shown to exhibit the characteristics of surfactant-enhanced spreading (Stoebe et al., 1997b). Spreading has been studied on liquid substrates (Stoebe et al., 1997a; Svitova et al., 2001a).

Wagner et al. (1999a) investigated the spreading rate of trisiloxane surfactants on low energy surfaces as a function of temperature. At room temperature, the trisiloxane with six ethoxylate groups was found to spread the fastest. At 40 °C, M(D′E_8OCH_3)M and a commercial superwetting agent were found to prevail. Svitova et al.

(1998) measured the contact angle of aqueous droplets of $M(D'E_nOCH_3)M$ for $n = 6$, 8, and 12 on highly hydrophobic surfaces at concentrations below the critical aggregation concentration (CAC). The surfactant structures formed by aqueous solutions of $M(D'E_6OH)M$, $M(D'E_8OH)M$, and $C_{12}E_3$ on graphite have been probed using atomic force microscopy (Svitova et al., 2001b). For substrates of varying surface energy, Grant et al. (1998) have studied the adsorption of C_mE_n surfactants while Dong et al. (2004) have investigated $M(D'E_nOH)M$ for $n = 6$, 8, and 12. Similar structures are found between the two classes for similar values of n.

Svitova et al. (1996) measured the dynamic surface tension of trisiloxane and alkyl polyethoxylate surfactants at high concentrations using the drop volume method. Solutions containing vesicles were found to reduce the surface tension faster than micellar solutions. Gentle and Snow (1995) determined the equilibrium surface tension below the CAC for $M(D'E_nOH)M$ for $n = 4$–16. They found the surface adsorption to be the same for n less than 16 implying that the maximum packing concentration is determined by the hydrophobe over this range.

The wetting behavior of neat trisiloxane and alkyl polyethoxylate droplets on substrates of varying surface energy has been studied using ellipsometry (Cazabat et al., 1994; Tiberg and Cazabat, 1994). Cazabat and coworkers found that trisiloxane droplets form bilayers on low energy substrates and wedge or sand pile-shaped precursor films on high energy substrates. Ruckenstein (1996) suggests that the formation of the bilayer on a hydrophobic surface is driven by short-range attractive forces between the hydrophobe of the surfactant and the substrate.

Churaev et al. (2001a) found good agreement between experimental data and their hydrodynamic calculations when the disjoining pressure was included. The authors suggest that thick wetting films, which are stabilized by vesicles and electrostatic forces, are the equilibrium shapes formed by aqueous trisiloxane droplets. Evidence was found for a bilayer structure. Churaev et al. (2001b) demonstrated the removal of silicone oils from hydrophobic surfaces using aqueous solutions of $M(D'E_8)M$. Nikolov et al. (2002) propose that superspreading is due to an enhanced Marangoni effect. Additional authors (Rafaï et al., 2002; Rafaï and Bonn, 2005) have also proposed that the Marangoni effect is the driving force behind superspreading.

Kumar et al. (2003) measured the rate of adsorption of trisiloxane surfactants ($M(D'E_nOH)M$ for $n = 4$, 8, and 12) at the liquid–vapor interface for bulk concentrations below the CAC. The authors concluded that the adsorption rates were not large enough to maintain the high surface concentrations necessary for superspreading. The direct adsorption of molecular aggregates instead of monomer may supply the interfaces with the needed surfactant. Kumar et al. (2006) used infrared spectroscopy to infer the arrangement $M(D'E_8OH)M$ and $C_{12}E_8$ molecules at the surface of a methyl-terminated alkylsilane SAM. The trisiloxane surfactant was shown to be more effective at removing water from the interface and its cylindrical shape was cited as the dominant reason. Solutions above and below the CAC were considered.

A number of authors have conducted molecular dynamics simulations with all-atom force fields to investigate the wetting behavior of pure droplets on solid substrates. Hautman and Klein (1991) studied the wetting of self-assembled monolayers by water. Striking agreement was seen between the microscopic contact angles obtained by simulation and the experimental macroscopic values. Mar and Klein (1994) examined the behavior of a sessile drop consisting of 80 hexadecane molecules on a methyl-terminated alkylthiol monolayer. Fan and Cagin (1995) investigated the wetting properties of crystalline polymer surfaces by droplets of water and methylene iodide. Recently, the dewetting of a water film on a damaged alkylsilane SAM has been simulated by Lane et al. (2008).

Werder et al. (2003) studied the wetting of graphite by water. The authors determined the Lennard-Jones parameters for the carbon–oxygen interaction that reproduced the macroscopic contact angle of 86°. The initial configuration of the droplet and motion of the lattice were shown to have no significant influence on the equilibrium contact angle. Lundgren et al. (2002) investigated the wetting of a single layer of hexagonal graphite by water. Using 900 water molecules the authors found that the water droplet formed a microscopic contact angle of 83°. An aqueous droplet of 30 wt% ethanol was shown to give a 30° decrease in the contact angle, which is consistent with the experimental findings. This is one of the first simulation studies to explore the effects of amphiphiles on wetting.

Previous molecular simulations aimed at investigating the wetting of solid substrates by surfactant-laden droplets have used generic interaction potentials. McNamara et al. (2001) considered cylindrical droplets and showed that surfactants could enhance wetting when the solvophobic tail group embedded itself into the solid substrate. While such a behavior may be possible for some substrates, it is unlikely for surfaces formed from self-assembled monolayers and rigid, atomically smooth solids like graphite. Shen et al. (2005) carried out a comparative study of linear and T-shaped surfactants. Results for two sets of interaction coefficients were reported. For the reference set the authors found that the droplet with T-shaped surfactants spread significantly more than the linear case. When the interaction between the solvent and the solvophilic groups was reduced the extent of spreading was found to be similar for both systems with more surfactant found at the solid–liquid interface for the T-shaped case. The adsorption isotherms for the linear surfactants have been determined (Tomassone et al., 2001a, b). Kim et al. (2006) considered linear surfactants only. The authors found that the spreading rate was strongly influenced by the strength of the interaction between the tail group of the surfactant and the substrate. The present study is a continuation of these past works but with real force fields whose results may be compared to the experiment.

Molecular simulations are limited to nanometer length scales and nanosecond time scales. Because of this it is not possible to test every mechanism that has been proposed to explain superspreading. For instance, the drop cannot be made large enough to study the role of vesicles. Similarly, the Marangoni effect cannot be seen for nanoscopic systems. However, a few of the proposed mechanism can be examined. Specifically, by studying trisiloxane and alkyl polyethoxylate surfactant-laden droplets we can learn about how the wetting behavior is affected by the orientation of the surfactant at the spreading edge, the affinity of each surfactant for the substrate, and whether or not the spreading edge forms a structure like a bilayer. Because the bilayer is a small structure (two molecules in the vertical direction) it can readily be reproduced by a simulation.

2. Simulation methodology

In the first set of simulations the wetting of graphite by spherical water and surfactant-laden droplets was studied. The drops for these simulations were constructed by extracting a spherical cluster from a large simple cubic lattice of randomly orientated water molecules arranged at ambient liquid density. Surfactant molecules, either $M(D'E_4OH)M$ or $C_{12}E_4$, were arranged at the liquid–vapor interface in the all-trans configuration with their hydrophiles inserted into the drop and their hydrophobes in air.

A spherical water droplet composed of 9997 molecules has a radius of roughly 4 nm. The inverse surface concentration at maximum packing for $M(D'E_4OH)M$ is 53.4 $Å^2$/molecule (Kumar et al., 2003). At this concentration there would be 377 surfactant molecules on the surface of the droplet. To keep the interfacial tensions low as the droplets spreads the surface concentrations must remain high. To ensure that this happens an additional 98 molecules were added. The critical aggregate concentration for $M(D'E_4OH)M$ is

0.11 mole/m^3 (Kumar et al., 2003). If the bulk concentration of the droplet were at the CAC the number of surfactant molecules in the droplet would be CAC $\times V \times N_A = (0.11\,\text{mole/m}^3)(4/3\pi R^3)N_A = 0.02$ molecules, where V is the volume of the droplet and N_A is Avogadro's number. There were no surfactant molecules in the bulk of the droplets for the initial simulations. For the trisiloxane system the solution concentration is 54.6 wt%, which is much larger than the typical 1 wt% used in experimental superspreading studies. The $C_{12}E_4/H_2O$ droplet was constructed in a similar manner. With the CAC for $C_{12}E_4$ being 0.05 mole/m^3 (Hsu et al., 2000) the number of molecules in bulk should be 0.01. In order to compare the two simulations 475 surfactant molecules were placed on the liquid–vapor interface of the droplet. We point out that because the number of surfactant molecules for the trisiloxane and alkyl polyethoxylate systems were the same, the alkyl polyethoxylate systems (having the larger maximum packing concentration) had a less crowded interface at initialization than the trisiloxane systems. We did not study alkyl polyethoxylate systems with crowded interfaces.

The graphite substrate was arranged in the same manner as Werder et al. (2003). Water and surfactant interacted with graphite through a Lennard-Jones interaction with the parameters for the water-graphite interaction taken from Werder et al. (2003), which specifically considered the SPC/E model for water. The separation distance between the two graphene layers is 3.41 Å. The carbon–carbon bond length is 1.421 Å. The atoms composing the substrate were fixed in space for all but one simulation.

Two different simulation codes were used in this work. The spherical droplet simulations were carried out at constant number of molecules, system volume, and temperature using a self-written code. The velocity Verlet method was used to perform the numerical integration of the equations of motion. All bond lengths were kept fixed using RATTLE (Andersen, 1983). The temperature was maintained at 298.15 K using a Nosé–Hoover thermostat with a relaxation time of 15 fs. The timestep was 2 fs. The SPC/E interaction potential (Berendsen et al., 1987) was used for water while the OPLS-UA force field (Jorgensen et al., 1984; Jorgensen, 1986) and a force field for polydimethylsiloxane (Sok et al., 1992) were used for the surfactants. The OPLS combining rules were used. The interaction between any pair of atoms in the same molecule which are separated by three or fewer bonds was excluded. Short-range interactions were cutoff at 10 Å. Open boundary conditions were used. An external potential was used to contain vapor molecules. The simulations were run on DataStar at the San Diego Supercomputer Center.

The fast multipole method (FMM) with four levels of spatial refinement was used to compute long-range interactions (Greengard and Rokhlin, 1987; Kurzak and Pettitt, 2005). The number of terms retained in the multipole expansion, p, was 5. A multiple time stepping scheme was used where the far-field coefficients were only updated once every 10 time steps. The neighbor lists were updated with the same frequency. These choices were shown to give a root-mean-square error in the force of less than 1% on average. Similar parameters have been used elsewhere (Lupo et al., 2002).

A spatial decomposition scheme was employed (Plimpton, 1995). The message-passing interface (MPI) was used to accomplish the parallelization. Load balancing was done manually at the beginning of each job step by choosing a domain shape that minimized the void space. During early times when the droplet is approximately spherical a cubic volume was used. As the droplet spread, the number of spatial sub-domains in the direction normal to the substrate was reduced while those in the transverse directions were increased.

A second set of simulations were conducted using cylindrical instead of spherical droplets. The advantage of the cylindrical shape over that of a sphere is that more solvent particles can be simulated for the same surface concentration of surfactant and CPU time. Cylindrical droplet wetting simulations were carried out for water and three surfactant solutions: $M(D'E_4OH)M/H_2O$, $MDM'E_4OH/H_2O$, and $C_{12}E_4/H_2O$. The number of water molecules and surfactant molecules in each case was 12,000 and 245, respectively. Only differences in simulation methodologies between the spherical and cylindrical droplet wetting runs are described here.

The molecular dynamics simulations (Frenkel and Smit, 2002) for the cylindrical nanodroplets were carried out at constant number of molecules, system volume, and temperature using the third-party code NAMD (Phillips et al., 2005). The Verlet method was used to perform the numerical integration of the equations of motion for the surfactant molecules and chains of the monolayer while SETTLE (Miyamoto and Kollman, 1992) was used for water. All bond lengths in the surfactant and monolayer were kept fixed using SHAKE (Ryckaert et al., 1977). Periodic boundary conditions in three dimensions were used. The box dimensions were $L_x = 34.43$ Å, $L_y = 397.60$ Å, and $L_z = 250.00$ Å. The particle-mesh Ewald (PME) technique (Darden et al., 1993; Essmann et al., 1995) was used to account for long-range interactions with the smallest number of grid points per direction being 0.88 Å^{-1}. The timestep was 2 fs. The temperature was maintained at 298.15 K by applying a Langevin thermostat, with a damping coefficient of 0.5 ps^{-1}, to non-hydrogen atoms.

The substrate was composed of a self-assembled monolayer with 80 chains in the x-direction and 8 chains in the y-direction (for details see Halverson et al., 2009). The mole fraction of $HOCH_2$-terminated chains was $\chi_p = 0.25$. This corresponds to a water contact angle of 75.9° making the substrate for these simulations less hydrophobic than graphite. Stoebe et al. (1996) showed that the maximum spreading rate for $M(D'E_4OH)M/H_2O$ occurred at a surfactant concentration of 2 wt% on a SAM with a water contact angle of 66°.

A third set of simulations investigated the wetting of methyl- and hydroxyl-terminated SAMs by neat or nearly water-free trisiloxane droplets. These simulations were conducted in the same manner as the previous cases. Results were obtained at room temperature and 450 K.

3. Results and discussion

3.1. Spherical droplets

The equilibrium contact angle of pure water on graphite was computed. The water–carbon Lennard-Jones parameters of $\sigma_{CO} = 3.19$ Å and $\varepsilon_{CO} = 392.0$ J/mol were taken from Werder et al. (2003). Using a smoothed non-bonded potential with a cutoff of 1 nm, Werder et al. (2003) report a contact angle of 95.3° for a droplet composed of 2000 molecules. Later it was shown that for such systems the contact angle depends on the value of the truncation radius (Jaffe et al., 2004). Walther et al. (2004) find a value of 89.73° for a smoothed potential with a cutoff and 90.99° when full electrostatic interactions are taken into account using the smooth PME method. In the present work, where electrostatic interactions are computed directly using the FMM, a value of 89° was found. The accepted experimental value for a macroscopic drop (where the effect of line tension is negligible) is 86°.

The spherical droplet of water and trisiloxane was initialized with the surfactant molecules densely packed at the liquid–vapor interface. A short MD run of 20 ps was performed in vacuum to equilibrate the drop. At $t = 0$ of the wetting simulation, the equilibrated droplet was placed a few angstroms away from the graphite substrate. The system was then evolved according to the MD method at 298.15 K. A cross-sectional view of the final configuration of the simulation is shown in Fig. 3. The simulation was stopped after 1.1 ns because very little spreading was seen. The figure reveals that the interfaces are densely packed with surfactant. The inverse surface concentrations at the solid–liquid and liquid–vapor interfaces are 75 and 57 Å^2/molecule, respectively. The polyethoxylate chains are seen to be interacting with water while the trisiloxane hydrophobes

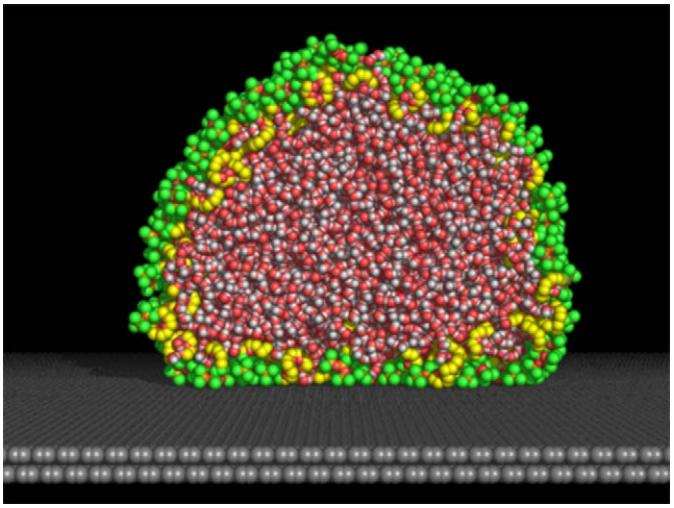

Fig. 3. Cross-sectional view of the final configuration of the trisiloxane/water droplet at 1.1 ns. Same coloring scheme as Fig. 1 with graphite as gray.

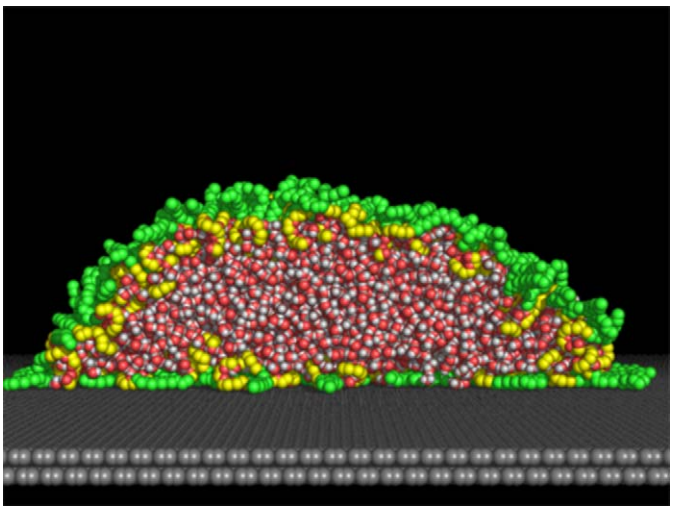

Fig. 4. Cross-sectional view of the final configuration of the alkyl polyethoxylate/water droplet at 1.3 ns. Same coloring scheme as Fig. 1 with graphite as gray.

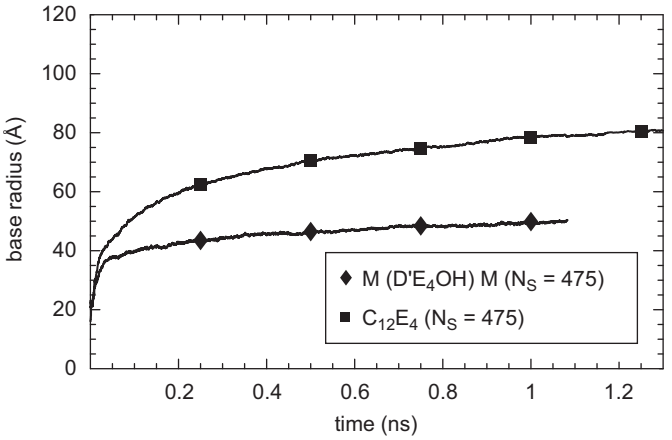

Fig. 5. Base radius versus time for the M(D′E$_4$OH)M/H$_2$O and C$_{12}$E$_4$/H$_2$O droplets.

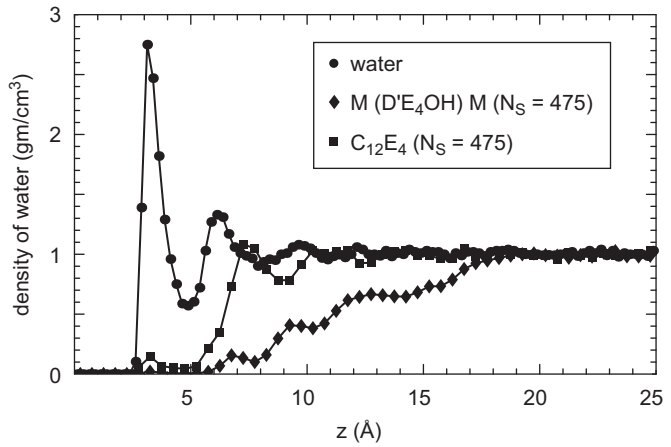

Fig. 6. Water density in the normal direction for spherical droplets of pure water, M(D′E$_4$OH)M/H$_2$O, and C$_{12}$E$_4$/H$_2$O. The top plane of atoms in the graphite lattice are located at $z = 0$.

are in air or in contact with the substrate. None of the surfactant molecules were seen to leave the interface and enter the bulk of the droplet during the simulation. The equilibrium contact angle of the droplet is larger than 90°. Clearly, superspreading was not observed and reasons for this will be discussed below.

The C$_{12}$E$_4$/H$_2$O droplet was initialized in the same manner as above. The droplet configuration at the final time step is shown in Fig. 4. The droplet is found to spread more than the trisiloxane case. The inverse surface concentrations at the solid–liquid and liquid–vapor interfaces are 134 and 63 Å^2/molecule, respectively. The final contact angle is approximately 55°.

For simulations of a pure droplet on a flat substrate the contact angle is found by fitting the time-averaged liquid–vapor boundary profile to a circle (de Ruijter et al., 1999). For a surfactant-laden droplet the approach is less obvious. However, because the droplets on average have the shape of a spherical cap the procedure of Kim et al. (2006) may be used. The base radius, r_B, is taken as the radius of a cylinder, which is aligned with the center-of-mass axis of the droplet, that contains 85% of the atoms that are within 10 Å of the substrate. The height, h, is taken as the height of a cylinder with a radius of 10 Å, which is aligned with the center-of-mass axis of the droplet, that contains 85% of the atoms that are between the substrate and h. The contact angle is determined by r_B and h through $\cos\theta = 1 - h/R$ and $(R-h)^2 = R^2 - r_B^2$, where R is the radius of the truncated sphere.

The extent of spreading of the two droplets is characterized by the change in base radius (Fig. 5). The base radius of the trisiloxane droplet changes very little with time after the first 100 ps of the simulation. The C$_{12}$E$_4$/H$_2$O droplet, which also begins as a sphere with a radius of 4 nm, is found to have a final base radius of 8 nm.

The water density in the normal direction is shown in Fig. 6. The edges of the droplets were ignored in calculating these profiles. For the pure water droplet, peaks are seen at $z = 3.1$ and 6.1 Å. These arise from water molecules adopting configurations at the solid–liquid interface that maximize the number of hydrogen bonds. The curve is in agreement with Fig. 9 of Werder et al. (2003). The trisiloxane surfactants are found to exclude water from the interface. However, this is largely due to the high initial surface concentration and the lack of spreading. The projected area of the trisiloxane group of a M(D′E$_4$OH)M molecule is approximately equivalent to the polyethoxylate head group of the molecule (Gentle and Snow, 1995). The bulk density of water is recovered at $z \approx 20$ Å. The C$_{12}$E$_4$ molecules are not as effective as the trisiloxanes at removing interfacial water. Because the alkyl polyethoxylate surfactants are

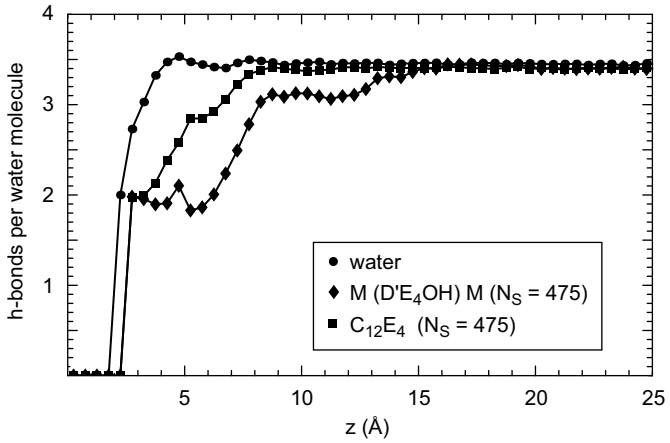

Fig. 7. Number of hydrogen bonds per water molecule in the normal direction for spherical droplets of pure water, M(D′E_4OH)M/H_2O, and $C_{12}E_4$/H_2O on graphite.

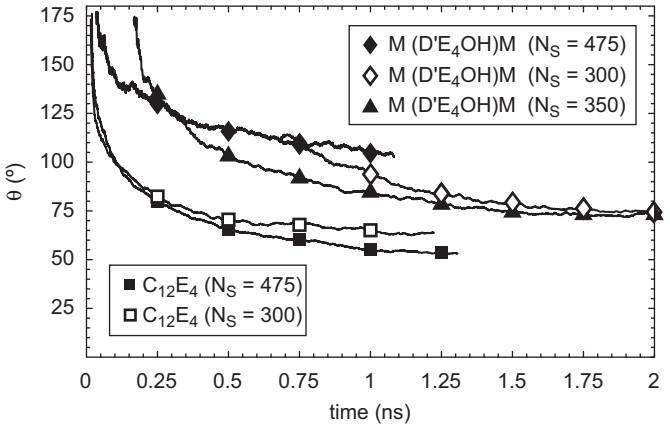

Fig. 8. Contact angle versus time for five surfactant-laden droplets on graphite. The number of water molecules was 9997 in all cases.

not as tightly packed, the density of water reaches its bulk value at $z \approx 7.0$ Å.

The number of hydrogen bonds per water molecule is shown in Fig. 7 as a function of the z-coordinate. According to the geometric definition of Martí (1999), two water molecules form a hydrogen bond if the oxygen–oxygen and oxygen–hydrogen separation distances are less than 3.6 and 2.4 Å, respectively. Furthermore, the angle between the vector formed by the oxygen atoms and the vector formed by the hydrogen atom and oxygen atom of the molecule of interest must be less than 30°. The same criteria was applied to determine the number of hydrogen bonds between water and surfactant. For the pure water droplet we find a bulk value of 3.5 hydrogen bonds per water molecule. In the vicinity of the hydrophobic solid the number of hydrogen bonds is found to decrease. In the region close to the substrate, water molecules are found to have more hydrogen bonds on average for the polyethyoxylate solution than for the trisiloxane case.

The M(D′E_4OH)M/H_2O droplet did not spread appreciably because there were too many molecules on the liquid–vapor interface. The initial inverse surface concentration for both surfactant droplets was 42 Å^2/molecule. This value is higher than the inverse maximum packing concentration for a planar monolayer of M(D′E_4OH)M, which is 54.3 Å^2/molecule (Kumar et al., 2003). The surfactant molecules at the interface prevent the droplet from changing its shape. The $C_{12}E_4$/H_2O droplet did spread appreciably because the initial surface concentration is very similar to its maximum packing concentration where the minimum in the liquid–vapor interfacial tension is found. The structural differences between the two surfactant molecules also play a role. The linear surfactants do not pack as tightly as the trisiloxanes for a given value of the surface concentration which leads to a less crowded interface. The maximum packing concentration of $C_{12}E_4$ at the liquid–vapor interface has been reported as 38 Å^2/molecule (Hsu et al., 2000) and 44 ± 3 Å^2/molecule (Lu et al., 2000). Based on experimental data (Kumar et al., 2003), the value of γ for this system at initialization is 43.5 mN/m.

To test the hypothesis that there was too much surfactant in the trisiloxane case, a new starting configuration was created by randomly removing 175 surfactant molecules from the droplet at t=0.7 ns. When this was done the droplet was found to spread more. The contact angle was found to decrease by 30° from $t = 0.7$ to 2 ns (open diamond symbols in Fig. 8). However, the final contact angle is comparable to the water contact angle of 89°. A third simulation was run where at initialization only 250 M(D′E_4OH)M molecules where placed on the surface and 100 molecules were randomly distributed throughout the bulk of the droplet. This gives an inverse surface concentration of 80.4 Å^2/molecule. In this case, the final value of θ was found to be 80°.

For the $C_{12}E_4$/H_2O case, an additional run was conducted with 300 molecules instead of 475. For this system the initial inverse surface concentration is 67.0 Å^2/molecule, which corresponds to a liquid–vapor interfacial tension of 60.7 mN/m. It can be seen from Fig. 8 that the equilibrium contact angle is higher than that of the original case. The $C_{12}E_4$/H_2O droplets appear to follow a classical wetting model where the droplet spreads until the forces at the three-phase contact line balance. Because the simulations are conducted with a fixed number of surfactants molecules, spreading ceases when the interfacial areas become large. It is expected that if more surfactant were added to the $N_S = 300$ droplet that additional spreading would occur.

The wetting behavior of a spherical droplet composed of 20,000 water molecules and 673 M(D′E_4OH)M molecules on a SAM with $\chi_p = 0.367$ was also studied. With five of the surfactant molecules initialized in the bulk of the droplet the initial inverse surface concentration was 67.7 Å^2/molecule. As in the previous cases very little spreading was seen. After 6.2 ns the temperature of the system was increased to 450 K. This caused several water molecules to escape from the droplet and act as a vapor. Additional spreading was seen but it was not dramatic.

3.2. Cylindrical droplets

Wetting simulations were conducted for M(D′E_4OH)M/H_2O, MDM′E_4OH/H_2O, and $C_{12}E_4$/H_2O in the form of cylindrical droplets. Each droplet was composed of 12,000 water molecules and 245 surfactant molecules. The same overall behavior was seen for the cylindrical droplets as for the spherical cases. That is, little spreading was observed. The final configurations of the M(D′E_4OH)M/H_2O and $C_{12}E_4$/H_2O droplets are shown in Fig. 9 at $t = 19.0$ ns. The radius and inverse surface concentration at $t = 0$ for each droplet were 5 nm and 44.2 Å^2/molecule, respectively.

The $C_{12}E_4$/H_2O droplet is found to have a lower center-of-mass position, z_{CM}, than the other surfactant-laden droplets (Fig. 10). This is because the initial surface concentration for this droplet is similar to the maximum packing concentration of $C_{12}E_4$ whereas for the hammer-like trisiloxane case the initial surface concentration is larger than its maximum packing concentration. The structure of the linear surfactants leads to a less crowded interface which allows for additional spreading. The MDM′E_4OH/H_2O droplet is found to have a similar final value of z_{CM} as compared to the M(D′E_4OH)M/H_2O droplet.

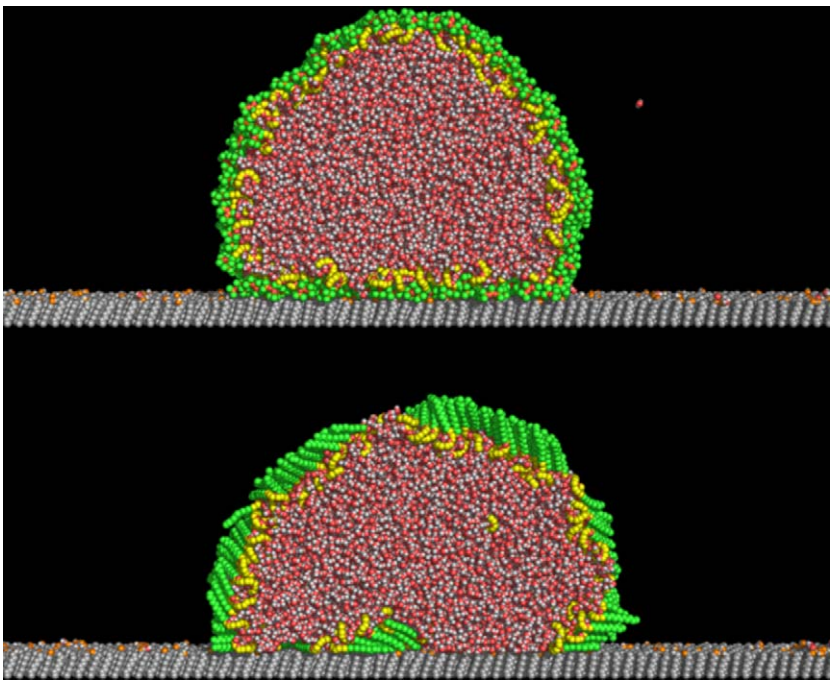

Fig. 9. Final configurations of cylindrical M(D′E_4OH)M/H_2O (top) and $C_{12}E_4$/H_2O (bottom) droplets at $t = 19$ ns on a self-assembled monolayer with a mole fraction of hydroxyl-terminated chains of $\chi_p = 0.25$.

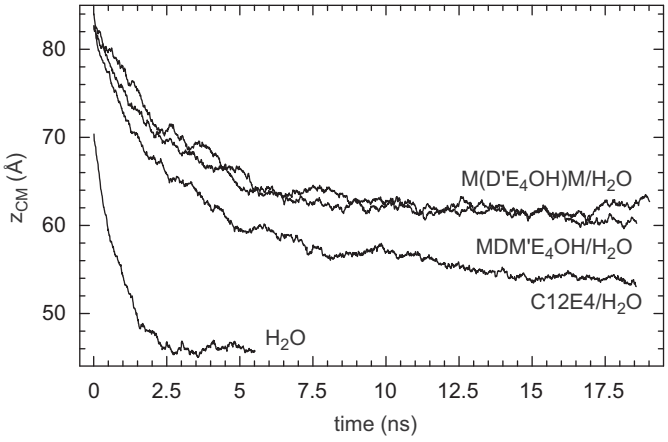

Fig. 10. Center-of-mass position versus time for water and three surfactant-laden droplets.

3.3. Neat surfactant droplets

Simulations of neat M(D′E_4OH)M droplets composed of 500 molecules on methyl- and hydroxyl-terminated SAMs have been conducted. In both cases the contact angle after 10 ns was found to be greater than 90°. The simulations were repeated with 2000 water molecules per drop. This was done because the experimentally determined spreading rates were shown to increase with humidity (Tiberg and Cazabat, 1994). With the addition of water and an increase in temperature to 450 K, the droplet on the hydrophobic substrate gave a layered structure (Fig. 11) and the droplet on the hydrophilic substrate gave a sand pile-shape (Fig. 12). Similar profiles at room temperature were found for M(D′E_8OH)M (Tiberg and Cazabat, 1994, Fig. 2a,d).

4. Conclusions

Molecular dynamics simulations were conducted to study of the wetting of hydrophobic substrates by droplets of aqueous superspreading and alkyl polyethoxylate surfactants solutions. While the $C_{12}E_4$ systems showed a behavior that is consistent with a simple wetting theory based on the Young equation, the trisiloxane systems showed a different behavior. For initial surface concentrations above the maximum packing concentration the M(D′E_4OH)M/H_2O and MDM′E_4OH/H_2O droplets did not spread appreciably. When the initial surface concentration was below the maximum packing concentration the M(D′E_4OH)M/H_2O droplet showed increased spreading but the final contact angle was still comparable to the water contact angle.

The failure of the simulated trisiloxane drops to spread is disappointing, and several possible explanations are available. The simplest excuse would be that the drop was too small or the time interval studied was too short. However, the numerous simulations of drop dynamics cited in the introduction typically involve comparable calculations with drops of 10,000–100,000 atoms evolving over nanoseconds and were quite capable of addressing spreading dynamics. Furthermore, the polyethoxylate simulations reported here involve similar length and time scales and are in accord with the experiments. A second possibility is that the form or the strength of the interactions used in the trisiloxane case were incorrect. Indeed, chemical groups involving silicon have received rather less modeling attention than the hydrocarbon components of the alkyl polyethoxylates and more guesswork and extrapolation is required. We have experimented with altering the numerical parameters in the trisiloxane interactions, with little change in the results, but the functional form was fixed and the OPLS and Lorentz–Berthelot combination rules limit the range of variation.

The key problem, we feel, is the need to maintain a substantial surfactant concentration on the liquid–vapor and solid–liquid interfaces as the drop spreads and its surface area increases. A physical drop in equilibrium maintains a balance between bulk and

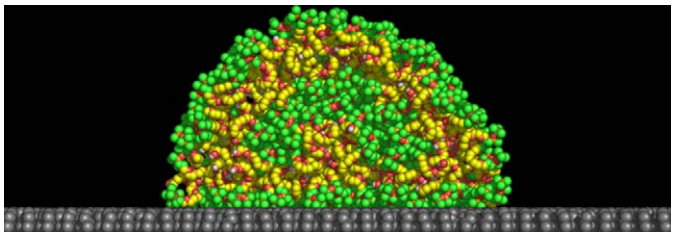

Fig. 11. Cross-sectional view of a neat droplet of 500 M(D′E$_4$OH)M molecules at equilibrium on a methyl-terminated SAM at 450 K. The 2000 water molecules in the simulation are not shown. Same coloring scheme as Fig. 1 with the SAM shown in gray.

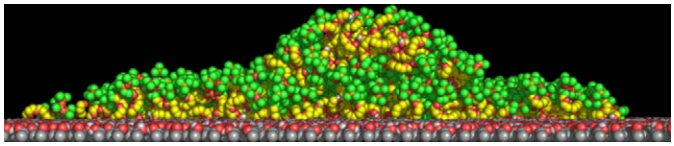

Fig. 12. Same as Fig. 11 except for a hydroxyl-terminated SAM.

interfacial surfactant dictated by the appropriate isotherm, and if a macroscopic drop begins to spread along a substrate there is an adequate supply of bulk surfactant to accommodate the growing interfacial area. The present simulations are of course severely constrained in scale, and it is not feasible to include any significant number of bulk surfactant molecules. Furthermore, even if we began with a much larger simulated drop which could contain enough additional surfactant for this purpose, the time scale for their molecular diffusion to the interface would likely be prohibitive, given our finite computational resources. These considerations led to our simulating a drop having a high initial interfacial concentration of surfactant, depicted in Fig. 3, which suggests an alternative possible explanation. The surfactant-coated interface in this figure is suggestive of a water drop coated by a membrane, which would have to deform considerably if the drop spreads, and such a deformation would be initiated by thermal fluctuations which accentuate the relative motion of the surfactant molecules. The length scales associated with thermal fluctuations is an increasing function of system size, and it may be that the fluctuations on drops of the simulated size are just too small.

Notation

h	height of a spherical cap, Å
k_θ	valence potential coefficient, kcal/mol/rad^2
L	length of the simulation cell, Å
N_A	Avogadro's number
N_S	number of surfactant molecules in the droplet
p	number of terms retained in the FMM
q_i	partial atomic charge, e
r_B	base radius of a spherical cap, Å
R	radius of droplet, nm
t	time
V	volume of droplet
V_i	dihedral potential function coefficients, kcal/mol
z_{CM}	z-component of the center-of-mass position, Å

Greek letters

γ	interfacial tension, mN/m
ε_{ii}	Lennard-Jones parameter, J/mol
θ	contact angle or valence angle, deg
θ_0	equilibrium valence angle, deg
σ_{ii}	Lennard-Jones parameter, Å
χ_p	mole fraction of hydroxl-terminated chains in the SAM

Subscripts

CM	center-of-mass
m	number of methyl and methylene groups
n	number of ethylene oxide groups
SL	solid–liquid
SV	solid–vapor

Acknowledgments

This work was funded by a NSF IGERT Graduate Research Fellowship in Multiscale Phenomena of Soft Materials, and it was supported in part by the National Science Foundation through a large resource allocation (LRAC) on DataStar at the San Diego Supercomputer Center. One of us (J.H.) would like to thank J. Kurzak for a discussion at the 11th Annual SDSC Summer Institute which led to a performance enhancement of our FMM implementation.

Appendix A. Bilayer formation of an aqueous trisiloxane solution

The trisiloxane droplets which were initialized with a surface concentration larger than the maximum packing concentration showed little spreading for both the spherical and cylindrical cases. It was argued that the crowded interfaces of these droplets prevented the rearrangement of surfactant molecules into a bilayer at the spreading edge (as observed experimentally). To test the hypothesis that the trisiloxane molecules are capable of forming a bilayer if given enough freedom for molecular rearrangement we have conducted an additional simulation of an aqueous M(D′E$_4$OH)M solution on a graphite substrate. The system was initialized with 126 surfactant molecules randomly distributed away from the substrate and 63 molecules arranged in a monolayer at the substrate–solution interface (Fig. 13). The total number of water molecules was 8829. The box dimensions were $L_x = 72.47$ Å, $L_y = 56.61$ Å, and $L_z = 143.41$ Å. The temperature was increased uniformly in steps of 25 K from 298.15 to 375 K over the first 35 ns of the simulation. NAMD was used with the same algorithm choices as for the cylindrical droplets.

During the first 10 ns of the simulation most of the surfactant away from the substrate had agglomerated to form an amorphous

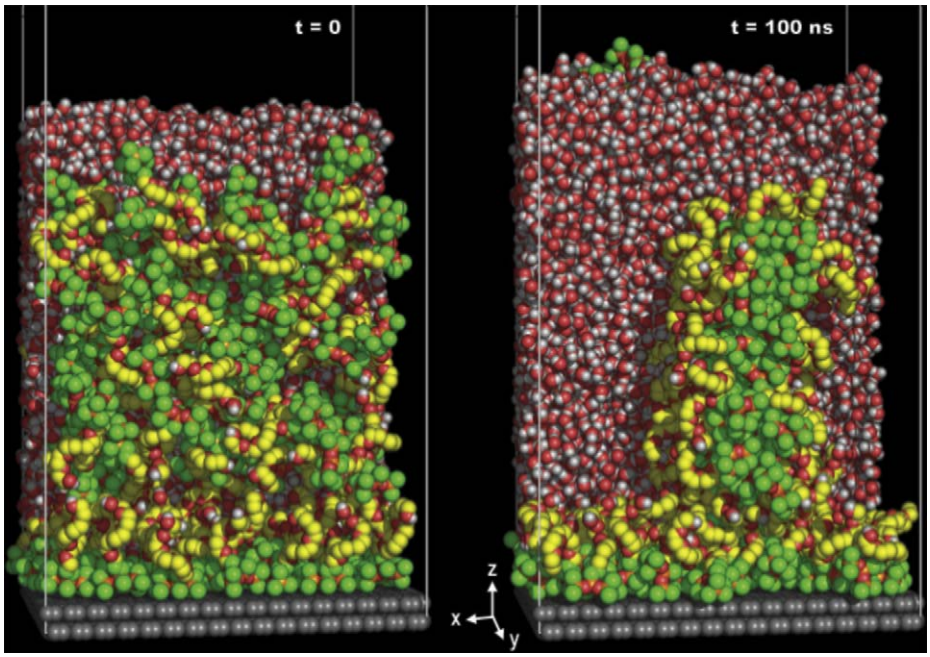

Fig. 13. (Left) At $t = 0$, trisiloxane surfactant molecules are randomly distributed throughout an aqueous solution, which is in contact with a graphite substrate. A surfactant monolayer was arranged on the substrate. (Right) At $t = 100$ ns, the surfactant molecules are found to self-assemble into a bilayer. Water molecules have been removed from the front half of each configuration for visual clarity.

Table 1
Bond lengths and valence angles.

Bond	Length (Å)	
O–H[a]	1.000	
O–H[b]	0.945	
CH_2–O[b,e]	1.430	
CH_2–CH_2[c]	1.516	
CH_2–O[c]	1.410	
CH_2–CH_2[e]	1.530	
CH_2–CH_3[e]	1.530	
CH_2–Si[d]	1.880	
Si–CH_3[d]	1.880	
Si–O[d]	1.600	
Valence	k_θ	θ_0 (°)
H–O–H[a]	–	109.47
H–O–CH_2[b]	110.02	108.5
O–CH_2–CH_2[b]	100.09	108.0
CH_2–O–CH_2[c]	124.20	112.0
O–CH_2–CH_2[c,e]	100.00	112.0
CH_2–CH_2–CH_2[c,e]	124.20	112.0
CH_2–CH_2–CH_3[e]	124.20	112.0
CH_2–CH_2–Si[d]	124.20	112.0
CH_2–Si–CH_3[d]	99.94	109.5
CH_2–Si–O[d]	99.94	109.5
Si–O–Si[d]	28.28	144.0
O–Si–O[d]	188.98	109.5
CH_3–Si–O[d]	99.94	109.5
CH_3–Si–CH_3[d]	99.94	109.5

The valence potential energy is given by $U = (k_\theta/2)(\theta - \theta_0)^2$. k_θ is given in units of kcal/mol/rad^2.
[a]Water.
[b]Alcohol group.
[c]Ethoxylate group.
[d]Trisiloxane group.
[e]Hydrocarbon.

Table 2
Dihedral angle parameters for the surfactant molecules.

Dihedral	V_1	V_2	V_3
H–O–CH_2–CH_2[a]	12.550	0.0	0.0
O–CH_2–CH_2–CH_2[a,b]	0.702	−0.212	3.060
O–CH_2–CH_2–O[b]	0.702	−0.212	3.060
CH_2–O–CH_2–CH_2[b,d]	4.744	−1.398	2.140
O–CH_2–CH_2–CH_2[b,d]	1.411	−0.271	3.145
CH_2–CH_2–CH_2–CH_2[d]	1.411	−0.271	3.145
CH_2–CH_2–CH_2–CH_3[d]	1.411	−0.271	3.145
CH_2–CH_2–CH_2–Si[d]	1.411	−0.271	3.145
CH_2–CH_2–Si–CH_3[d]	1.411	−0.271	3.145
CH_3–CH_2–Si–O[d]	1.411	−0.271	3.145
CH_2–Si–O–Si[c]	0.0	0.0	1.801
Si–O–Si–CH_3[c]	0.0	0.0	1.801
O–Si–O–Si[c]	0.0	0.0	1.801

The dihedral potential energy is given by $U = (V_1/2)(1 + \cos\phi) + (V_2/2)(1 - \cos 2\phi) + (V_3/2)(1 + \cos 3\phi)$. V_i are given in units of kcal/mol.
[a]Alcohol group.
[b]Ethoxylate group.
[c]Trisiloxane group.
[d]Hydrocarbon.

aggregate. Two surfactant molecules went to the liquid–vapor interface. At $t = 23$ ns, the bottom of the aggregate was found to be separated from the head groups of the surfactants at the solid–liquid interface by roughly 1 nm. From 23 to 30 ns, the aggregate was found to move toward and eventually attach to the monolayer. A distinct bilayer was found at $t = 45$ ns and this structure was found to be stable for an additional 55 ns. The final configuration is shown in Fig. 13. The approximate height and thickness of the bilayer are 6.5 and 2.5 nm, respectively. A similar behavior was found for a $C_{12}E_4$ system where the bilayer height and thickness were 5.5 and 3.0 nm.

The result of the trisiloxane simulation supports the idea (in the introduction) that bilayer formation occurs in the trisiloxane systems and that such structures may be a key ingredient in enhanced spreading. It also supports the claim that future simulations should consider larger droplets with lower initial surface concentrations and surfactant reservoirs in the bulk. The surfactant molecules in such a system would have enough freedom to rearrange as necessary and to sustain spreading by adsorbing at the interfaces. Finally, this result lends further support for the parameterization of our force field.

Table 3
Lennard-Jones and Coulomb parameters for water and the surfactant molecules.

Non-bonded i–i	σ_{ii} (Å)	ε_{ii}	q_i (e)
H–H[a]	0.0	0.0	0.4238
O–O[a]	3.166	650.2	−0.8476
H–H[b]	0.0	0.0	0.265
O–O[b]	3.070	711.8	−0.700
CH_2–CH_2[b]	3.905	493.9	0.435
CH_2–CH_2[c]	3.905	493.9	0.0
O–O[c]	3.047	817.8	−0.580
Si–Si[d]	3.385	2448.0	0.300
CH_3–CH_3[d]	3.790	753.2	0.0
O–O[d]	2.960	849.3	−0.300
CH_2–CH_2[d]	3.905	493.9	0.0
CH_3–CH_3[e]	3.905	732.5	0.0
C–C[f]	3.214	236.3	0.0

The Lennard-Jones potential energy is given by $U = 4\varepsilon_{ij}[(\sigma_{ij}/r_{ij})^{12} - (\sigma_{ij}/r_{ij})^{6}]$. ε_{ij} are given in units of J/mol.

The Coulomb interaction is $(4\pi\varepsilon_0)^{-1} q_i q_j r_{ij}^{-1}$.

[a]Water.
[b]Alcohol group.
[c]Ethoxylate group.
[d]Trisiloxane group.
[e]Hydrocarbon.
[f]Graphite.

Appendix B. Force field for MD simulations

The alkyl polyethoxylate surfactants are described by the OPLS-UA force field while the trisiloxane surfactants are described by this and a second force field (Sok et al., 1992). To ensure electroneutrality of the trisiloxane group the two terminal Si atoms were assigned partial charges of 0.15e while the central Si atom remained at 0.3e. To prevent hydrogen bonds from forming between the hydrogen atom of the hydroxyl group with the oxygen atom of the adjacent ethoxylate group (i.e., a 1–5 interaction) the dihedral potential coefficient for the H–O–C–C angle was increased by a factor of 10. The TraPPE-UA force field, which was not used in this study, solves this problem by introducing a repulsive interaction between the two atoms (Stubbs et al., 2004) (Tables 1–3).

References

Ananthapadmanabhan, K.P., Doddard, E.D., Chandar, P., 1990. A study of the solution, interfacial and wetting properties of silicone surfactants. Colloids and Surfaces 44, 281–297.

Andersen, H.C., 1983. RATTLE: a velocity version of the shake algorithm for molecular-dynamics calculations. Journal of Computational Physics 52 (1), 24–34.

Berendsen, H.J.C., Grigera, J.R., Straatsma, T.P., 1987. The missing term in effective pair potentials. Journal of Physical Chemistry 91 (24), 6269–6271.

Cazabat, A.M., Fraysse, N., Heslot, F., Levinson, P., Marsh, J., Tiberg, F., Valignat, M.P., 1994. Pancakes. Advances in Colloid and Interface Science 48, 1–17.

Churaev, N.V., Esipova, N.E., Hill, R.M., Sobolev, V.D., Starov, V.M., Zorin, Z.M., 2001a. The superspreading effect of trisiloxane surfactant solutions. Langmuir 17, 1338–1348.

Churaev, N.V., Ershov, A.P., Esipova, N.E., Hill, R.M., Sobolev, V.D., Zorin, Z.M., 2001b. Application of a trisiloxane surfactant for removal oils from hydrophobic surfaces. Langmuir 17, 1349–1356.

Darden, T.A., York, D.M., Pederson, L.G., 1993. Particle mesh Ewald: an $N\log(N)$ method for Ewald sums in large systems. Journal of Chemical Physics 98 (12), 10089–10092.

de Gennes, P.G., 1985. Wetting: statics and dynamics. Reviews of Modern Physics 57 (3), 827–863.

DeLano, W.L., 2002. The PyMOL Molecular Graphics System. DeLano Scientific, Palo Alto, CA, USA.

de Ruijter, M.J., Blake, T.D., De Coninick, J., 1999. Dynamic wetting studied by molecular modeling simulations of droplet spreading. Langmuir 15 (22), 7836–7847.

Dong, J., Mao, G., Hill, R.M., 2004. Nanoscale aggregate structures of trisiloxane surfactants at the solid–liquid interface. Langmuir 20 (7), 2695–2700.

Essmann, U., Perera, L., Berkowitz, M.L., Darden, T., Lee, H., Pederson, L., 1995. A smooth particle mesh Ewald method. The Journal of Chemical Physics 103 (19), 8577–8593.

Fan, C.F., Cagin, T., 1995. Wetting of crystalline polymer surfaces: a molecular dynamics simulation. Journal of Chemical Physics 103 (20), 9053–9061.

Frenkel, D., Smit, B., 2002. Understanding Molecular Simulation. second ed. Academic Press, London. pp. 63–105.

Gentle, T.E., Snow, S.A., 1995. Absorption of small silicone polyether surfactants at the air/water surface. Langmuir 11 (8), 2905–2910.

Gradzielski, M., Hoffmann, H., Robisch, P., Ulbricht, W., Grüning, B., 1990. Aggregation behaviour of silicone surfactants in aqueous solutions. Tenside, Surfactants, Detergent 27 (6), 366–379.

Grant, L.M., Tiberg, F., Ducker, W.A., 1998. Nanometer-scale organization of ethylene oxide surfactants on graphite, hydrophilic silica, and hydrophobic silica. Journal of Physical Chemistry B 102 (22), 4288–4294.

Greengard, L., Rokhlin, V., 1987. A fast algorithm for particle simulations. Journal of Computational Physics 73 (2), 325–348.

Halverson, J.D., Maldarelli, C., Couzis, A., Koplik, J., 2009. Atomistic simulations of the wetting behavior of nanodroplets of water on homogeneous and phase separated self-assembled monolayers. Langmuir, submitted for publication.

Hautman, J., Klein, M.L., 1991. Microscopic wetting phenomena. Physical Review Letters 67 (13), 1763–1766.

He, M., Hill, R.M., Lin, Z., Scriven, L.E., Davis, H.T., 1993. Phase behavior and microstructure of polyoxyethylene trisiloxane surfactants in aqueous solution. The Journal of Physical Chemistry 97 (34), 8820–8834.

Hill, R.M., 1998. Superspreading. Current Opinion in Colloid and Interface Science 3, 247–254.

Hill, R.M., He, M., Davis, H.T., 1994. Comparison of the liquid-crystal phase-behavior of 4 trisiloxane superwetter surfactants. Langmuir 10 (6), 1724–1734.

Hsu, C.-T., Shao, M.-J., Lin, S.-Y., 2000. Adsorption kinetics of $C_{12}E_4$ at the air–water interface: adsorption onto a fresh interface. Langmuir 16 (7), 3187–3194.

Jaffe, R.L., Gonnet, P., Werder, T., Walther, J.H., Koumoutsakos, P., 2004. Water–carbon interactions 2: calibration of potentials using contact angle data for different interaction models. Molecular Simulation 30 (4), 205–216.

Jorgensen, W.L., Madura, J.D., Swenson, C.J., 1984. Optimized intermolecular potential functions for liquid hydrocarbons. Journal of the American Chemical Society 106 (22), 6638–6646.

Jorgensen, W.L., 1986. Optimized intermolecular potential functions for liquid alcohols. Journal of the American Chemical Society 90 (7), 1276–1284.

Kim, H.-Y., Yin, Q., Fichthorn, K.A., 2006. Molecular dynamics simulation of nanodroplet spreading enhanced by linear surfactants. The Journal of Chemical Physics 125 (17), 174708.

Knoche, M., 1994. Organosilicone surfactant performance in agricultural spray applications: a review. Weed Research 34, 221–239.

Kumar, N., Couzis, A., Maldarelli, C., 2003. Measurement of the kinetic rate constants for the adsorption of superspreading trisiloxanes to an air/aqueous interface and the relevance of these measurements to the mechanism of superspreading. Journal of Colloid and Interface Science 267, 272–285.

Kumar, N., Maldarelli, C., Couzis, A., 2006. An infrared spectroscopy study of hydrogen bonding and water restructuring as a trisiloxane surfactant adsorbs onto an aqueous–hydrophobic surface. Colloids and Surfaces A: Physicochemical and Engineering Aspects 277, 98–106.

Kunieda, H., Taoka, H., Iwanaga, T., Harashima, A., 1998. Phase behavior of polyoxyethylene trisiloxane surfactant in water and water–oil. Langmuir 14 (18), 5113–5120.

Kurzak, J., Pettitt, B.M., 2005. Massively parallel implementation of a fast multipole method for distributed memory machines. Journal of Parallel and Distributed Computing 65 (7), 870–881.

Lane, J.M.D., Chandross, M., Lorenz, C.D., Stevens, M.J., Grest, G.S., 2008. Water penetration of damaged self-assembled monolayers. Langmuir 24 (11), 5734–5739.

Li, X., Washenberger, R.M., Scriven, L.E., Davis, H.T., 1999a. Phase behavior and microstructure of water/trisiloxane E-12 polyoxyethylene surfactant/silicone oil systems. Langmuir 15 (7), 2267–2277.

Li, X., Washenberger, R.M., Scriven, L.E., Davis, H.T., 1999b. Phase behavior and microstructure of water/trisiloxane E-6 and E-10 polyoxyethylene surfactant/silicone oil systems. Langmuir 15 (7), 2278–2289.

Lu, J.R., Thomas, R.K., Penfold, J., 2000. Surfactant layers at the air/water interface: structure and composition. Advances in Colloid and Interface Science 84 (1–3), 143–304.

Lundgren, M., Allan, N.L., Cosgrove, T., George, N., 2002. Wetting of water and water/ethanol droplets on a non-polar surface: a molecular dynamics study. Langmuir 18 (26), 10462–10466.

Lupo, J.A., Wang, Z., McKenney, A.M., Pachter, R., Mattson, W., 2002. A large scale molecular dynamics simulation code using the fast multipole algorithm (FMD): performance and application. Journal of Molecular Graphics and Modelling 21 (2), 89–99.

Mar, W., Klein, M.L., 1994. A molecular-dynamics study of n-hexadecane droplets on a hydrophobic surface. Journal of Physics: Condensed Matter 6, A381–A388.

Martí, J., 1999. Analysis of the hydrogen bonding and vibrational spectra of supercritical model water by molecular dynamics simulations. The Journal of Chemical Physics 110 (14), 6876–6886.

McNamara, S., Koplik, J., Banavar, J.R., 2001. Simulations of surfactant-enhanced spreading. In: Alexandrov, V.N., Dongarra, J.J., Juliano, B.A., Renner, R.S., Tan, C.J.K. (Eds.), Proceedings of the International Conference on Computational Sciences—Part I, London, pp. 551–559.

Miyamoto, S., Kollman, P.A., 1992. SETTLE: An analytical version of the SHAKE and RATTLE algorithm for rigid water models. Journal of Computational Chemistry 13 (8), 952–962.

Nikolov, A.D., Wasan, D.T., Chengara, A., Koczo, K., Policello, G.A., Kolossvary, I., 2002. Superspreading driven by Marangoni flow. Advances in Colloid and Interface Science 96, 325–338.

Phillips, J.C., Braun, R., Wang, W., Gumbart, J., Tajkhorshid, E., Villa, E., Chipot, C., Skeel, R.D., Kale, L., Schulten, K., 2005. Scalable molecular dynamics with NAMD. Journal of Computational Chemistry 26 (16), 1781–1802.

Plimpton, S., 1995. Fast parallel algorithms for short-range molecular dynamics. Journal of Computational Physics 117 (1), 1–19.

Rafaï, S., Sarker, D., Bergeron, V., Meunier, J., Bonn, D., 2002. Superspreading: aqueous surfactant drops spreading on hydrophobic surfaces. Langmuir 18, 10486–10488.

Rafaï, S., Bonn, D., 2005. Spreading of non-Newtonian fluids and surfactant solutions on solid surfaces. Physica A 358, 58–67.

Ruckenstein, E., 1996. Effect of short-range interactions on spreading. Journal of Colloid and Interface Science 179, 136–142.

Ryckaert, J.P., Ciccotti, G., Berendsen, H.J.C., 1977. Numerical-integration of Cartesian equations of motion of a system with constraints: molecules-dynamics of n-alkanes. Journal of Computational Physics 23 (3), 327–341.

Schwartz, E.G., Reid, W.G., 1964. Surface-active agents: their behavior and industrial use. Industrial and Engineering Chemistry 56, 26–31.

Shen, Y., Couzis, A., Koplik, J., Maldarelli, C., Tomassone, M.S., 2005. Molecular dynamics study of the influence of surfactant structure on surfactant-facilitated spreading of droplets on solid surfaces. Langmuir 21, 12160–12170.

Sok, R.M., Berendsen, H.J.C., van Gunsteren, W.F., 1992. Molecular dynamics simulation of the transport of small molecules across a polymer membrane. The Journal of Chemical Physics 96 (6), 4699–4704.

Stoebe, T., Lin, Z., Hill, R.M., Ward, M.D., Davis, H.T., 1996. Surfactant-enhanced spreading. Langmuir 12, 337–344.

Stoebe, T., Lin, Z., Hill, R.M., Ward, M.D., Davis, H.T., 1997a. Superspreading of aqueous films containing trisiloxane surfactant on mineral oil. Langmuir 13, 7282–7286.

Stoebe, T., Hill, R.M., Ward, M.D., Davis, H.T., 1997b. Enhanced spreading of aqueous films containing ionic surfactants on solid substrates. Langmuir 13 (26), 7276–7281.

Stoebe, T., Lin, Z., Hill, R.M., Ward, M.D., Davis, H.T., 1997c. Enhanced spreading of aqueous films containing ethoxylated alcohol surfactants on solid substrates. Langmuir 13, 7270–7275.

Stubbs, J.M., Potoff, J.J., Siepmann, J.I., 2004. Transferable potentials for phase equilibria. 6. United-atom description for ethers, glycols, ketones, and aldehydes. The Journal of Physical Chemistry B 108 (45), 17596–17605.

Svitova, T., Hill, R.M., Smirnova, Y., Stuermer, A., Yakubov, G., 1998. Wetting and interfacial transitions in dilute solutions of trisiloxane surfactants. Langmuir 14 (18), 5023–5031.

Svitova, T., Hoffmann, H., Hill, R.M., 1996. Trisiloxane surfactants: surface/interfacial tension dynamics and spreading on hydrophobic surfaces. Langmuir 12 (7), 1712–1721.

Svitova, T.F., Hill, R.M., Radke, C.J., 2001a. Spreading of aqueous trisiloxane surfactant solutions over liquid hydrophobic substrates. Langmuir 17 (2), 335–348.

Svitova, T., Hill, R.M., Radke, C.J., 2001b. Adsorption layer structures and spreading behavior of aqueous non-ionic surfactants on graphite. Colloids and Surfaces A: Physicochemical and Engineering Aspects 183, 607–620.

Tiberg, F., Cazabat, A.M., 1994. Spreading of thin films of ordered nonionic surfactants: origin of the stepped shape of the spreading precursor. Langmuir 10, 2301–2306.

Tomassone, M.S., Couzis, A., Maldarelli, C.M., Banavar, J.R., Koplik, J., 2001a. Molecular dynamics simulation of gaseous–liquid phase transitions of soluble and insoluble surfactants at a fluid interface. The Journal of Chemical Physics 115 (18), 8634–8642.

Tomassone, M.S., Couzis, A., Maldarelli, C., Banavar, J.R., Koplik, J., 2001b. Phase transitions of soluble surfactants at a liquid–vapor interface. Langmuir 17, 6037–6040.

Wagner, R., Wu, Y., Czichocki, G., von Berlepsch, H., Rexin, F., Perepelittchenko, L., 1999a. Silicon-modified surfactants and wetting: II. Temperature-dependent spreading behaviour of oligoethylene glycol derivatives of heptamethyltrisiloxane. Applied Organometallic Chemistry 13 (3), 201–208.

Wagner, R., Wu, Y., von Berlepsch, H., Rexin, F., Rexin, T., Perepelittchenko, L., 1999b. Silicon-modified surfactants and wetting: III. The spreading behaviour of equimolar mixtures of nonionic trisiloxane surfactants on a low-energy solid surface. Applied Organometallic Chemistry 13 (9), 621–630.

Walther, J.H., Werder, T., Jaffe, R.L., Gonnet, P., Bergdorf, M., Zimmerli, U., Koumoutsakos, P., 2004. Water–carbon interactions III: the influence of surface and fluid impurities. Physical Chemistry Chemical Physics 6, 1988–1995.

Werder, T., Walther, J.H., Jaffe, R.L., Halicioglu, T., Koumoutsakos, P., 2003. On the water–carbon interaction for use in molecular dynamics simulations of graphite and carbon nanotubes. Journal of Physical Chemistry B 107 (6), 1345–1352.

Zhu, S., Miller, W.G., Scriven, L.E., Davis, H.T., 1994. Superspreading of water–silicone surfactant on hydrophobic surfaces. Colloids and Surfaces A: Physicochemical and Engineering Aspects 90 (1), 63–78.